XL CILAMCE
IBERO-LATIN AMERICAN CONGRESS ON COMPUTATIONAL METHODS IN ENGINEERING
NOVEMBER 11-14, 2019
Praiamar Natal Hotel & Convention Natal, RN-BRAZIL

TOPOLOGY OPTIMIZATION OF CONTINUUM TWO-DIMENSIONAL STRUCTURE UNDER VOLUME CONSTRAINT

Higo L. S. Nascimento
Rafael B. S. Araújo
leo.higo@hotmail.com
bezerraescossia@gmail.com
Federal University of Rio Grande do Norte, University Campus, Department of Mechanical Engineering
Lagoa Nova. Zip-Code: 59072-970. Natal-RN. Brazil.

Abstract. This work presents the Topology Optimization Method where the objective is to minimize compliance with lateral and volume constraints of a rib from aircraft wings profile leading edge. The problem is solved by a Topology Optimization Method technique, formulated as finding the best material distribution into the domain. The static problem is solved with the Finite Element Method were the structural response is given as nodal displacements. The Optimality criteria are based in the power-law approach, also known as Solid Isotropic Material with Penalization that uses a "fictitious" density to represent the material distribution into each finite element that defines the elastic properties of isotropic porous material. The solution is implemented with a didactic algorithm. No linear programming is used and a heuristic updating scheme is used as standard optimality criteria. Besides, sensitivity and densities filters are used to minimize the occurrence of numerical instabilities: checkerboards, mesh-dependencies, and local minima. The results are evaluated in three criteria: first, the occurrence of these instabilities and filter performance, second the convergence and implementation time and the last one a brief comparison with the literature and a general analysis of the results.

Keywords: Topology Optimization, Finite Elements, Wing profile, Rib, Unmanned Aerial Vehicle

1 Introduction

The Topological Optimization Method (TOM) is a category of structural optimization, which originated from layout optimization and parametric and shape optimizations, respectively. The first steps of structural optimization were introduced in the late 19th century, with Maxwell's work in 1872 in which he sought the smallest volume for uniaxial structures subjected to loading. In 1904 Michel continued Maxwell's work with its structures that are still cited in modern Topological Optimization theory. Michel designed lattice structures in search of the smallest volume, observing the tensions in the bars for each load case [1].

In the mid-1980s, the results of shape and parametric optimizations began to be questioned as they presented major problems when changing the topology. With the need to improve shape optimization, topology optimization (OT), Bendsøe, and Kikuchi emerged in the late 1990s. material represents, for each iteration, the solution of equilibrium equations [1].

Therefore, according to Porto and Pavanello [2] the idea is that topological optimization is used initially and then employed one of the classical methods of shape or parametric optimization. This second step will be performed faster and more efficiently, since it is already part of an optimal topology and is already very close to the exact one. Or as approached by Simonetti [1]: Olhoff in 1991 used topology as a "preprocessor" of shape and parametric optimizations giving these much better end results.

Topological optimization is already widespread today and is used in many commercial software. Among the present models, according to Simonetti [1] the OT can be classified as: the MOT from a discrete medium and from a continuous medium. In this work topological optimization is employed with the discretization of a continuous element with the use of finite elements to determine the optimal topology of a leading-edge rib profile of an aircraft in order to minimize flexibility considering prescribed volumes.

2 Topological Optimization Method

TOM is defined as the search for material distribution within a fixed domain, in which an objective function is minimized while a set of constraints is satisfied. The formulation of the problem begins by defining a parameterized artificial composite material and obtaining a relationship between these parameters and the constitutive properties of artificial microstructures for the solution of the optimal problem [2]. Artificial density loses its physical properties during iterations and becomes a mathematical variable used purely to obtain the solution.

The distribution of this porous material characterizes the SIMP (Simple Isotropic Material with Penalization) method shown in Equation (1) is based on the works of Sigmund [3], Andreassen and Clausen et al. [4]

$$E_k(x_k)=E_{min}+x_k^{\eta}(E_0-E_{min}),\ x_k \in [0,1] \tag{1}$$

Where E_k and E_0 are Young's modulus of the element and material respectively. E_{min} is a minimum value for Young's modulus used to avoid singularities in the stiffness matrix, x_k is the density of the element and η the penalty exponent.

2.1 Numerical Instabilities

Checkboard instability

The application of the SIMP method together with the Finite Element Method (FEM) discretization leads to the occurrence of numerical instabilities, a theme that has been well studied in the optimization area. The very common case in TOM is the checkboard or chess board instability is characterized by the presence of rapidly alternating regions between voids and solids, which resembles a chess board as shown in Figure 1 [2].

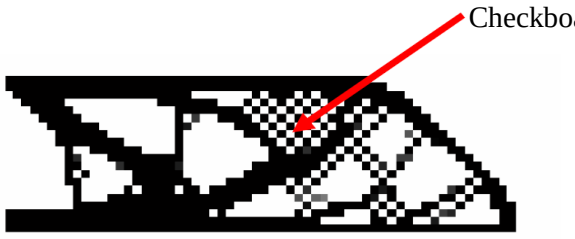

Figure 1. Checkboard instabilities [2].

According to Simonetti [1], the chessboard is the result of discretization made by the FEM. The board has greater stiffness than fully solid regions so this setting remains in the final result as a possible "optimum". However, this result is not consistent with reality, the stiffness is the result of the numerical instability [1] [5]. One of the ways to avoid this phenomenon is precisely the use of filters that prevent the sudden change of density in the results by evaluating the neighborhood of the elements, usually in this work represented by r_{min}.

Mesh dependency

According to Guilherme [6], mesh dependence is the problem of not qualitatively obtaining the same result for different mesh sizes or domain discretization. Figure 2 illustrates the mesh dependency. It can be seen that increasing the number of elements for a simple beam problem that has the effect of a point load has made the result increasingly complex: initially the presence of board instability, after that non-smooth contours in the voids and finally a complex geometry.

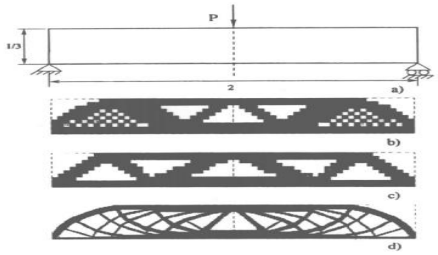

Figure 2. Mesh dependency [6].

2.2 Filters

Filters are heuristic methods used to solve numerical instability problems, used to ensure the existence of the solution and to avoid chessboard formations and mesh dependence [7].

The two filters used in this work are sensitivity and density filters. The first acts on the derivative of flexibility and the second directly on density. The sensitivity filter transforms the density derivative according to Equation (2) [4].

$$\frac{\widehat{\partial c}}{\partial x_k} = \frac{1}{\max(\gamma, x_k)\sum_{i\epsilon N_k} H_{ki}} \sum_{i\epsilon N_k} H_{ki} x_i \frac{\partial c}{\partial x_i} \tag{2}$$

Where γ is a positive constant used to avoid possible divisions by zero, N_k is the number of elements in the vicinity of the k elements. H_{ki} is the weight factor that is determined by Equation (3).

$$H_{ki} = \max\left(0, r_{min} - \Delta(k,i)\right) \tag{3}$$

Where r_{min} is the filter range, $\Delta(k, i)$ is the distance between the k elements and the neighboring element i. This neighborhood scan with the weighing of the elements within a minimum radius is done to avoid sudden changes in density, as presented in the section on numerical instability problems. The density filter transforms the original density x_k according to Equation (4).

$$\tilde{x}_k = \left(1 / \sum_{i\epsilon N_k} H_{ki}\right) \sum_{i\epsilon N_k} H_{ki} x_i \tag{4}$$

3 Materials and methods

3.1 Objective function and optimal problem

In this work the objective function c is defined as the flexibility of the structure, that is, the inverse of stiffness. Flexibility is defined in the Equation (5).

$$c(\mathbf{x})=\mathbf{F}^{\mathbf{T}}\mathbf{U} \tag{5}$$

F and **U** are the global force and displacement vectors respectively. As with an element, equilibrium conditions in a global analysis are presented in Equation (6).

$$\mathbf{KU}=\mathbf{F} \tag{6}$$

K is the global stiffness matrix. Thus, substituting Equation (6) in equation (5) flexibility can be defined as a function of the stiffness matrix and displacements only, as presented in Equation (7), which is precisely the objective function under analysis.

$$c(\mathbf{x})=\mathbf{U}^{\mathbf{T}}\mathbf{KU} \tag{7}$$

The optimal problem can be determined by considering the equilibrium conditions, lateral density constraints (values between 0 and 1), as the prescribed volume as can be observed in Equation (8) which presents optimization problem. based on Andreassen and Clausen et al. [4].

$$\begin{aligned} \min_{\mathbf{x}} \quad & c(\mathbf{x})=\mathbf{U}^{\mathbf{T}}\mathbf{KU}=\textstyle\sum_{k=1}^{N} E_k(x_k)\mathbf{u}^{\mathbf{T}}\mathbf{ku} \\ \text{st.} \quad & fr(\mathbf{x})=V(\mathbf{x})/V_0 \\ & \mathbf{KU}=\mathbf{F} \\ & 0\leq\mathbf{x}\leq 1 \end{aligned} \tag{8}$$

Where, in addition to the variables already presented in this section, **u** and **k** are the local displacement vector and the stiffness matrix, respectively, E_k Young's modulus of the element, fr is the prescribed fraction, V is the constraint volume, V is the current volume, V_0 is the initial volume, **x** the density and N the number of elements.

3.2 Boundary Conditions

The profile under review is an USA35-B common in an Unmanned Aerial Vehicle (UAV) sized and staffed by AeroDesign competitions [8]. Loading conditions were determined by the Profili 2.22a software. The input parameter, in addition to the profile, was the Reynolds number at 383000 standard value for an aircraft intended to participate in the SAE (Society of Automotive Engineers) competition. The program provided the data that was used to determine the wing pressure distribution as well as the lowest and highest support angles.

Figure 3 shows the pressure distribution at 0º, case (a), lower lift configuration and at 9.5º, case (b), higher lift, chosen for analysis, in both cases the wind gust considered is vertical.

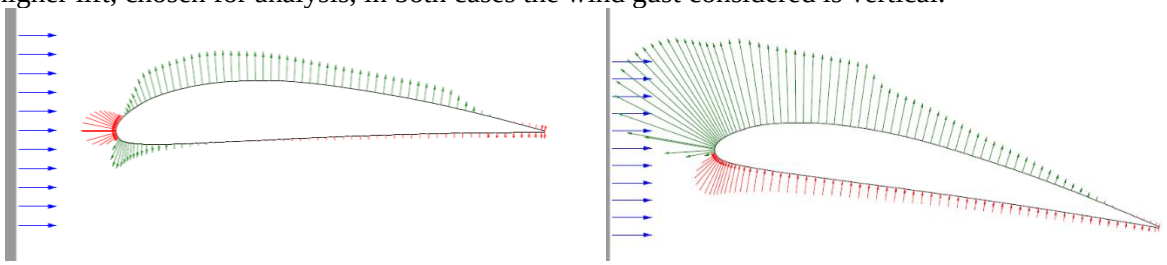

(a) (b)

Figure 3. Pressure distribution at (a) 0º and (b) 9.5º

The most heavily loaded region is just at the wing edge, as shown in Figure 3. Therefore, this is the region of interest for the application of the MOT. The leading-edge region of the wing profile with the highest loading is defined as 1/4 of the chord (total profile length), because it is in this region that the aerodynamic center is considered to be located. The aerodynamic center is an idealized point where the resulting forces and moments acting on the wing are located [9]. Therefore, the boundary conditions can be determined. according to the study by Xinxing, Wenjie et al. (2014) [10], Figure 4.

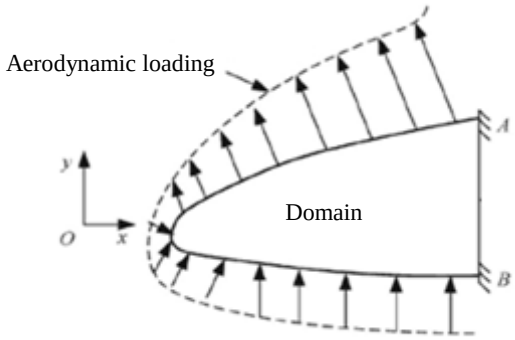

Figure 4. Wing edge profile [10] adapted.

The USA-35B profile was introduced into the algorithm by its coordinates in a 121x90 element domain with the insertion of voids as presented by Andreassen and Clausen et al. [4]. The coordinates used are from the database of the University of Illinois Aerospace Engineering Department [11].

Figure 5 shows the wing profile and the region of interest for determining rib geometry that is up to a quarter of the chord [9]. Excel software was used for plotting graphs.

Note that the vertical coordinates have negative real values, however the mesh numbering is done by positive integers. Therefore, it is necessary to perform a transformation in the field of coordinates.

The transformation of the coordinates was performed so that the final mesh had 121 elements in x and 90 elements in y, values chosen to maintain the proportionality of the profile. Therefore, the axes values of Figure 6 were transformed by the relationships shown in Equations (9) and (10), which were obtained by proportionality, direct to the horizontal axis, since the original values are on a unit scale, and a scale increased by 10 times for the vertical axis.

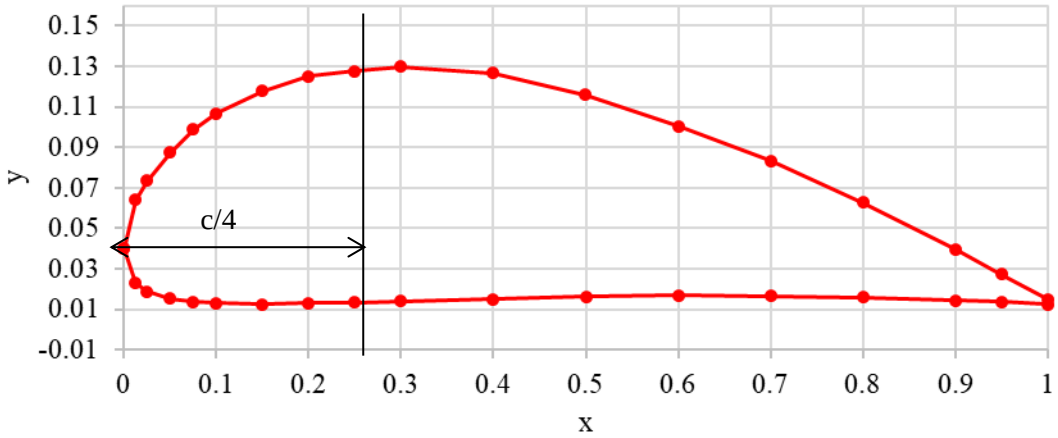

Figure 5. USA-35B Profile Coordinates [11] adapted

$$X=\left(\frac{nelx}{\left(\frac{nely}{3}\right)}\right)(x*nelx+1) \tag{9}$$

$$Y=(y*10)(nely+1) \tag{10}$$

Where X and Y are the horizontal and vertical coordinates after transformation, respectively, x and

y are the old coordinates. nelx and nely are the number of horizontal and vertical elements respectively.

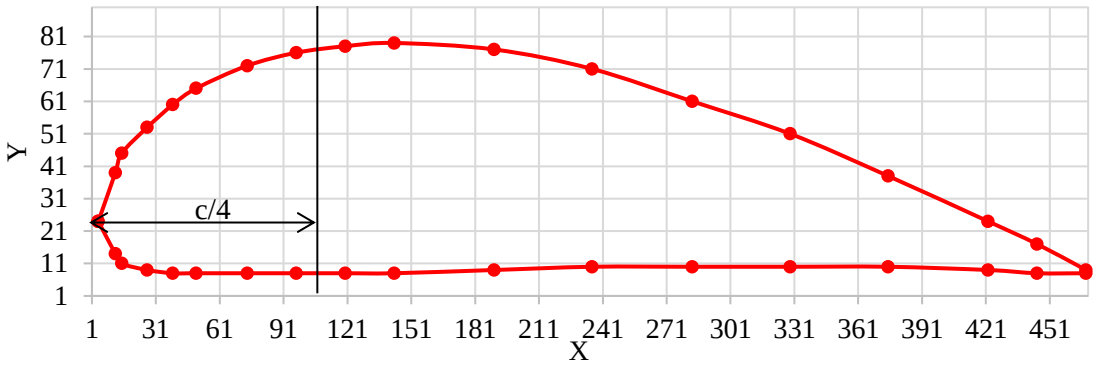

Figure 6. USA-35B Profile Coordinate Transformation.

Thus, with this transformation it is possible to determine the boundary conditions for the application in the algorithm. Distributed loading, for simplicity, is entered based on the approximation functions, see Figure 7 case (a). The start and end of each distributed load region is determined by Figure 7 case (b). The values of the forces were normalized as the largest load being the unit, the other values were reduced based on the approximation function.

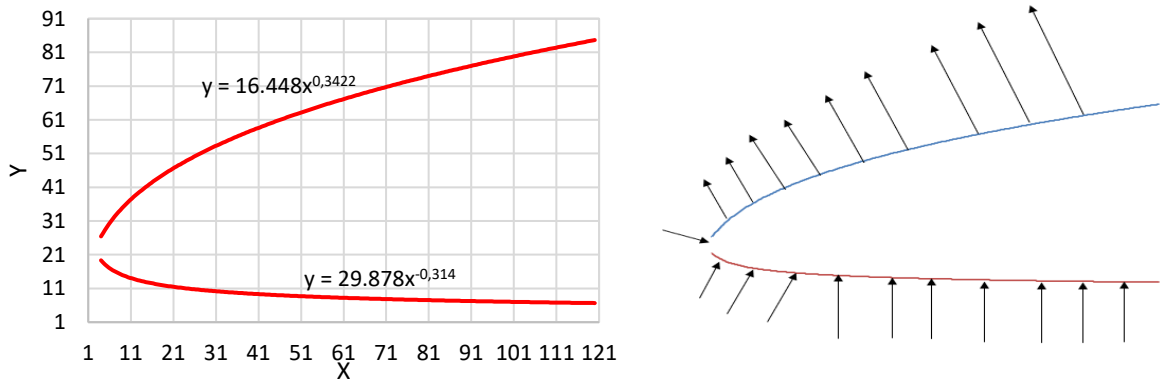

(a) (b)

Figure 7. Profile coordinates of the rope under 1/4, (a) approximation by two exponential functions and (b) load distribution.

3.3 Algorithm

The algorithm was implemented in the Matlab software, the same used by the models developed by Sigmund (2001) [3], Andreassen and Clausen et al. (2010) [4].

According to Andreassen and Clausen et al. (2010) [4], Matlab is an advanced programming language capable of solving numerous problems with simple code. However, compared to other languages such as C ++ and Fortran, it has a lower computational capacity mainly due to inadequate allocation and software tolerance for poor programming practices such as variable and vector misallocation. Therefore, the previous memory allocation is used, which is characterized by the sparse function.

Mesh and imput

The algorithm employed is the work of Andreassen and Clausen et al. (2010) [4] a didactic code that is based on the Sigmund [3] 99 line algorithm. Both models have the same implementation base, but the most current model enables the use of new filters, other solution methods, and better overall

performance. The calling function for the code is expressed in Equation (11).

$$\text{top88(nelx, nely, fr, penal, } r_{min}\text{, ft)} \tag{11}$$

Where nelx and nely are the horizontal and vertical element numbers respectively, fr is the volume fraction, penal is the penalty exponent, r_{min} is the filter for the minimum radius of filter neighborhood rating and "ft" specifies which filter: sensitivity (ft = 1) or density (ft = 2).
The model used for the domain are quadrilateral elements as shown in Figure 8 nodes are numbered relative to the left-to-right column of degrees of freedom in the order of "2n-1" where "2n" represents horizontal and vertical displacement. of node "n" respectively. This high mesh regularity can be harnessed in many ways to reduce the computational effort in looping.

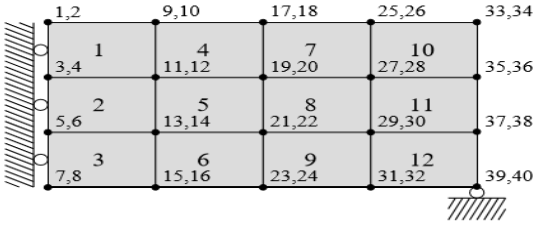

Figure 8. Model domain with 12 elements [4].

4 Results

The mesh used in the code was an 121x90 elements, prescribed volume ranges from 60% to 15% for optimal topology characterization, penalty exponent equal to 3 and r_{min} equal to 4% of the nelx, then equal to 5. Minimum radius and penalty exponent were determined based on the literature [3] [4].

The results shown in Figure 9 and Figure 10 represent only the wing edge profile support element, without the outer contour where the ribs (supports) are attached.

Figure 9 presents six results with the sensitivity filter. Results (a) and (b) show mesh dependence from the constraint and number of elements used. This effect is eliminated from case (c) with a prescribed volume of 40%. Convergence was relatively fast compared to the other examples. Just the case (f) which has a number of clashing interactions, which was caused because the constraint reached a limit of 15% and it can be seen that the inclined truss was not fully defined.

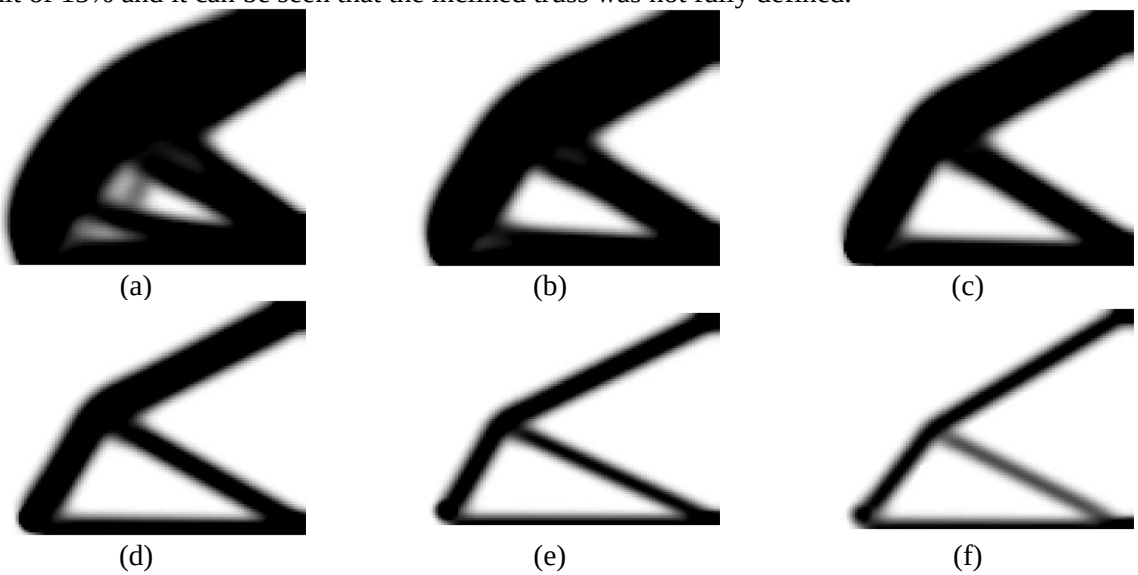

Figure 9. Results for with sensitivity filter, fr equal to (a) 60%, (b) 50%, (c) 40%, (d) 30%, (e) 20% e (f) 15%.

In the following tables (1) and (2) variables such as flexibility, c, and minimum radius (r_{min}) do not present units since the adopted model of the literature [4] applies a normalization dependent on the average and on the number of mesh elements. The same is true for the density which is treated as a pixel in the result figures and the material loads and properties normalized to unit values. This method of normalizing parameters is used to decrease the sensitivity of functions to variations in input parameters.

Table 1. Results with Sensitivity Filter.

Results	**nelx×nely**	**r_{min}**	**fr**	**ni**	**c**	**ch**	**t (s)**	**TI (s)**
(a)	121x90	5	60%	36	45.2563	0.010	19.693	0.547
(b)	121x90	5	50%	24	45.4878	0.009	13.087	0.545
(c)	121x90	5	40%	20	45.8674	0.009	12.716	0.636
(d)	121x90	5	30%	23	47.5662	0.009	13.129	0.571
(e)	121x90	5	20%	31	50.3360	0.009	16.383	0.528
(f)	121x90	5	15%	169	57.0130	0.010	82.382	0.487

Horizontal and vertical mesh elements, respectively, r_{min} is the neighborhood scan radius used in the filters, ni is the number of iterations, c is the flexibility, ch the condition of stop, t the convergence time and IT the convergence time by iteration.

It is noteworthy that the variation of the r_{min} not affect the result of the final topology, but because it results in a larger scan area in the vicinity of the elements considerably affects the convergence of the algorithm, so that from this section The minimum radius value is preset to 4% "nelx" as recommended by Andreassen and Clausen, et al. [4].

Figure 10 presents the results for the density filter which are similar as already noted in the previous examples. For the rib, the filter was more stable without mesh dependence for cases (a) and (b) and lower occurrence of gray regions. The result with 15% volume fraction, case (f), is also better defined

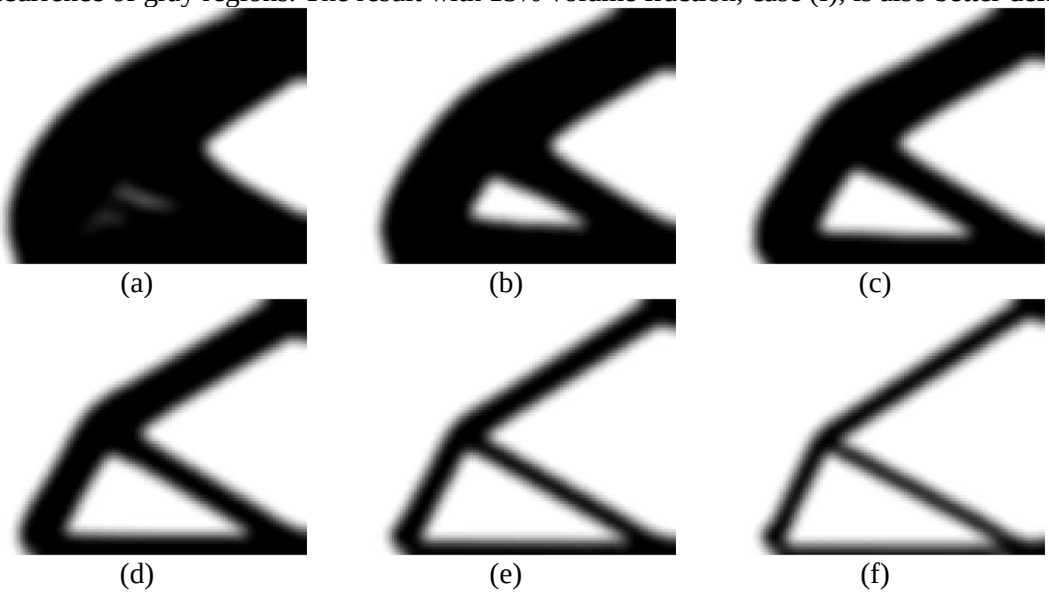

Figure 10. Results with density filter, fr equal to (a) 60%, (b) 50%, (c) 40%, (d) 30%, (e) 20% e (f) 15%

Table 2. Results with density filter.

Results	nelx×nely	r_{min}	fr	ni	c	ch	t (s)	TI (s)
(a)	121x90	5	60%	187	51,2636	0,010	121,870	0,651
(b)	121x90	5	50%	171	51,5240	0,008	115,969	0,678
(c)	121x90	5	40%	213	51,9413	0,008	142,822	0,671
(d)	121x90	5	30%	256	52,7409	0,006	235,948	0,922
(e)	121x90	5	20%	509	54,9361	0,009	388,069	0,762
(f)	121x90	5	15%	474	58,3318	0,006	340,007	0,717

The reduction in rib volume represents a significant optimization in the UAV, as total weight is an extremely important variable in its development. While reducing the volume of a naturally light element may seem unnecessary, a close to 85% reduction in a structure that is distributed across the wing results in an interesting mass reduction for a UAV design, even more so. models subject to aerodesign competitions as is the case analyzed in this paper.

Moreover, as already evaluated, this mass reduction improves important parameters such as lift, fuel consumption, engine choice, aerodynamic balance. Finally, the final geometry of the inner rib together with the wing bark at ¼ of the rope does not differ much from the model found in the literature [9] as seen in Figure 11.

Figure 11 shows the comparison of the wing leading edge profile tip. In case (b) in case (b) the result of Figure 10 case (d) as a 40% volume fraction. The contour of Figure 11 case (b) is used to represent the full profile, that is, the shell and the inner rib.

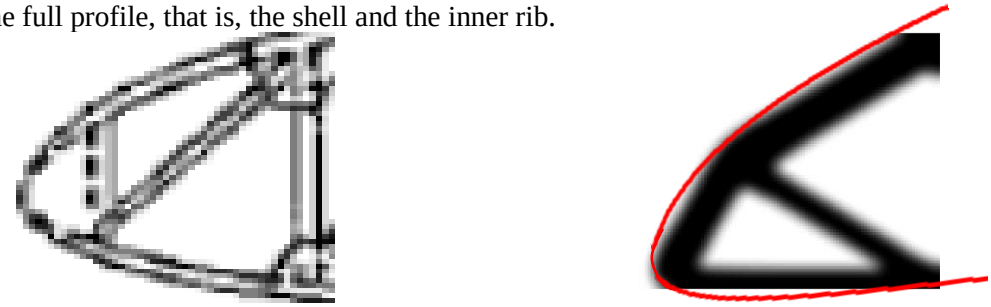

(a) (b)

Figure 11. Comparison between rib profile (a) literature (RODRIGUES, 2009) [8] adapted and (b) algorithm result for 20% of volume fraction with density filter.

5 Conclusions

The Topological Optimization Method (MOT) is a versatile and sophisticated optimization process determine an optimum. In this work the USA-35B profile was used because it is typical of small aircraft with a large wing area. The optimization result presented a topology similar to the model found in the literature. Furthermore, the validity of the application of MOT to light structures was discussed and it was concluded that the mass of a UAV, especially the subjects subjected to AeroDesign competitions, is an extremely important parameter, so the reduction of rib volume is a great desired because the overall weight of the structure is crucial in flight efficiency, glide height, lift, engine specification, fuel consumption and therefore the overall UAV price.

The filters used to determine the optimal topology significantly altered the results. It was concluded that the filter acting directly on the density presented a longer convergence time, but did not have mesh dependencies or chess boards for any case. The derivative filter (sensitivity) was faster in convergence in most cases and presented lower values for flexibility, on the other hand presented numerical instabilities such as mesh dependencies and undefined regions, gray.

Acknowledgements

The authors are grateful to UFRN, Department of Mechanical Engineering, for financial support and to João C. A. C. Júnior for acknowledge support.

References

[1]SIMONETTI, H. L. *Otimização topológica de estruturas bidimensionais*. Dissertação Mestrado – Universidade Federal de Ouro Preto. Escola de Minas. Departamento de Engenharia Civil. Programa de Pós Graduação em Engenharia Civil. Ouro Preto. 2009.

[2] PORTO, E. C. B.; PAVANELLO, R. Influência dos parâmetros de homogeneização sobre a solução estrutural topológica ótima. *8º Congreso Iberoamericano de Ingenieria Mecanica*, Cusco - Peru, v. 1, p. 1-9, 2007.

[3] SIGMUND, O. A 99 line topology optimization code written in Matlab. S*tructural and Multidisciplinary Optimization*, v. 21, n. 2, p. 120–127, 2001.

[4] ANDREASSEN, E.; CLAUSEN, A.; SCHEVENELS, M.; LAZAROV, B. S.; SIGMUND O. Efficient topology optimization in MATLAB using 88 lines of code. *Structural and Multidisciplinary Optimization*. v. 43, p. 1-16, 2010. ISSN 1.

[5] SANT'ANNA, H. M. *Otimização Topológica de Estruturas Bidimensionais Contínuas submetidas a restrições de flexibilidade e tensão*. Dissertação de Mestrado - UFRGS. Porto Alegre. 2002.

[6] GUILHERME, C. E. M. *Otimização topológica e cálculo do gradiente de forma para estruturas submetidas à restrição de fadiga*, Porto Alegre, v. Tese, 2006

[7] BOURDIN, B. Filters in topology optimization. International journal for numerical methods in engineering. *International journal for numerical methods in engineering*, v. 50, n. 9, p. 2143-2158, 2001.

[8]SAE BRASIL. *AeroDesign*, 2018. Disponivel em: <http://portal.saebrasil.org.br/programas-estudantis/sae-brasil-aerodesign>. Acesso em: 30 mai 2019.

[9] RODRIGUES, L. E. M. J. *Fundamentos da engenharia aeronáutica*. São Paulo: IFSP, 2009.

[10] XINXING,T.; WENJIE,G.; CHAO, S.; XIAOYON, Liu. Topology optimization of compliant adaptive wingleading edge with composite materials. *Chinese Journal of Aeronautics*, v. 27, n. 6, p. 1488-1494, 2014.

[11] UIUC. *The UIUC Airfoil Data Site*, 2019. Disponivel em: <https://mselig.ae.illinois.edu/ads/coord_database.html#U>. Acesso em: 30 mai 2019.